Impact of snow cover and topography on ultraviolet irradiance at the Alpine station of Briançon

Jacqueline Lenoble,[1,2] Arve Kylling,[3] and Irina Smolskaia[2,4]

Received 9 January 2004; revised 2 April 2004; accepted 4 June 2004; published 27 August 2004.

[1] The enhancement of the UV global irradiance due to snow cover on the ground has been observed at the station of Briançon, in a high-altitude Alpine valley. The analysis relies on a three-dimensional (3-D) model, using an elevation map of the area. Without snow, comparison with the results of a 1-D model shows no detectable effect of topography, within the uncertainty of modeling (2–3%). The 3-D model relates the enhancement due to snow to the altitude of the snow line. The enhancement is shown to depend on the snow distribution around the site and not on the topography itself. The enhancement was measured at Briançon for nine cloudless days in winter 2002. As expected, it increases with the decrease of the snow line. In erythemal UV the enhancement reaches a maximum of about 22% in the beginning of March, in agreement with the results of the 3-D model, assuming a snow albedo of 0.3 above the snow line and below the tree line and 0.8 above the tree line. Retrieving an effective surface albedo is a very challenging problem. Very small uncertainties in enhancement (±2%) lead to large uncertainties (±0.05) in effective albedo. Using the snow distribution with a contribution function does not give good results when the snow line is high; this is explained by the low resolution of the map with the rapid variation of the contribution near the site. *INDEX TERMS:* 0360 Atmospheric Composition and Structure: Transmission and scattering of radiation; 0394 Atmospheric Composition and Structure: Instruments and techniques; 3322 Meteorology and Atmospheric Dynamics: Land/atmosphere interactions; 3359 Meteorology and Atmospheric Dynamics: Radiative processes; *KEYWORDS:* ultraviolet, snow, mountain, radiative transfer

Citation: Lenoble, J., A. Kylling, and I. Smolskaia (2004), Impact of snow cover and topography on ultraviolet irradiance at the Alpine station of Briançon, *J. Geophys. Res.*, *109*, D16209, doi:10.1029/2004JD004523.

1. Introduction

[2] Whereas most surfaces, such as rocks, bare soil, vegetation, roads, or buildings, have a very low reflectance of a few percent in the ultraviolet range, snow-covered ground is highly reflecting, with a reflectance or albedo of about 80–90% for fresh clean snow and about 30–40% for old snow [*Blumthaler and Ambach*, 1988]; in this paper, we use the word albedo, more familiar to geophysicists than reflectance. It has been observed by several authors [*McKenzie et al.*, 1998; *Weihs et al.*, 1999; *Kylling et al.*, 2000a] that the presence of snow on the ground strongly enhances the ultraviolet (UV) global irradiance received at the Earth's surface. This enhancement is easily explained by the multiple reflections between the surface and the scattering atmosphere, using one-dimensional (1-D) radiative transfer theory [*Lenoble*, 1998]. The enhancement is much larger when the sky is cloudy than when it is clear, because of the increased atmospheric backscattering due to clouds. However, the impact of snow enhancement is particularly important for living organisms, including human beings, when the level of irradiance is high, that is, in cloudless conditions; we will limit our study to this situation.

[3] When the snow cover is not uniform, the impact of the snow distribution has been analyzed with three-dimensional (3-D) models, such as Spherical Harmonics Discrete Ordinate Method (SH-DOM) [*Degünther et al.*, 1998] or Monte Carlo [*Lenoble*, 2000; *Kylling and Mayer*, 2001]. All authors agree that areas more than 50 km away from the observation site can still contribute to a few percent of the enhancement. Measurements near the coastline between ocean and snow-covered terrain [*Smolskaia et al.*, 1999] have been discussed by *Mayer and Degünther* [2000] and have been reconciled with modeling by *Smolskaia* [2001].

[4] In mountainous regions the problem is made even more complex by the influence of topography; not only is the atmosphere optical depth not the same above the different zones, but topography can lead to shadowing of some surfaces or to multiple reflections between the slopes. The 3-D model used in the present study has earlier been used to investigate the effect of partial snow cover for a site in Tromsø, Norway [*Kylling and Mayer*, 2001].

[1] Laboratoire d'Optique Atmosphérique, Université des Sciences et Technologies de Lille, Lille, France.
[2] Equipe Interactions Rayonnement Solaire et Atmosphère, Université Joseph Fourier, Grenoble, France.
[3] Norwegian Institute for Air Research, Kjeller, Norway.
[4] Now at Institute for Meteorology and Climatology, Hannover University, Hannover, Germany.

0148-0227/04/2004JD004523

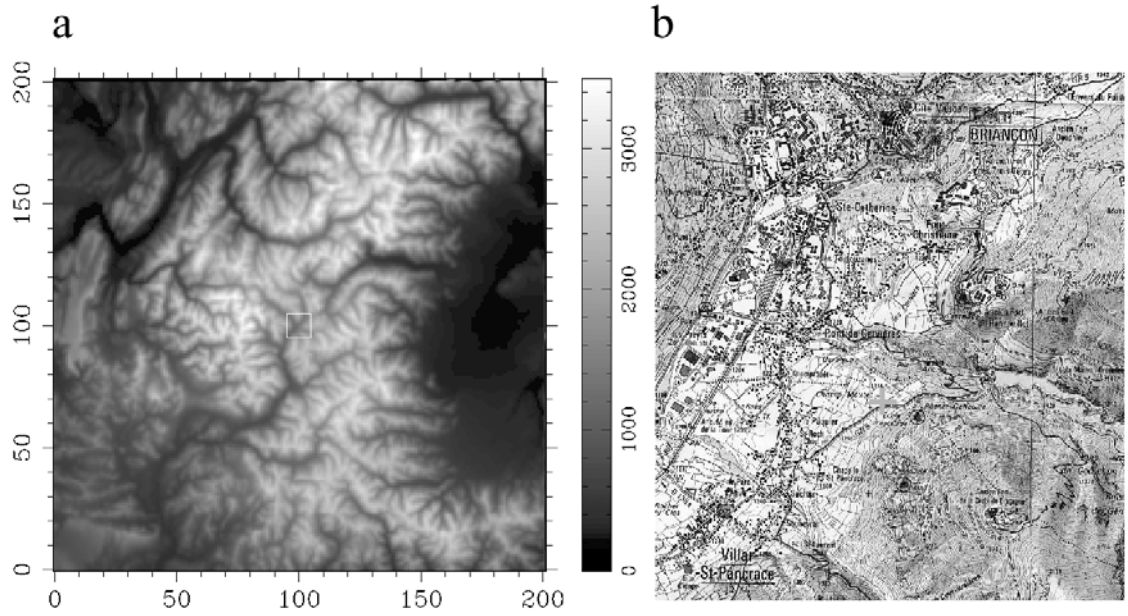

Figure 1. (a) Topographical map used in the 3-D model, in a domain of 201 × 201 km^2, centered at Briançon. (b) Map of Briançon site surroundings (Institut Géographique National).

[5] Our objective is to address the problem of the enhancement due to snow in the particular case of the site of Briançon in the French southern Alps. Briançon is located in a valley at about 1300 m above sea level, and measurements of spectral UV irradiance are regularly performed; they are analyzed with 3-D and 1-D models. Our conclusions, derived for the particular site of Briançon, should apply to other similar situations, that is, for places located in the bottom of a high-altitude valley. For stations located on a mountain summit, such as the Jungfraujoch or the Sonnblick, the results are certainly different.

[6] Section 2 presents the site of Briançon and the models used in this study; section 3 compares the results of 1-D and 3-D models in the absence of snow; section 4 presents the enhancement due to snow cover, modeled with a 3-D model, and analyzes the role of topography. In section 5 the enhancement observed during winter 2002 is presented and compared with the results predicted by a 3-D model. Finally, the retrieval of an effective surface albedo to be used in 1-D models is discussed in section 6. Section 7 summarizes our results.

2. Measurement Site and Models

[7] Briançon (44.90°N, 6.65°E) is a small town, located in the Durance Valley at the altitude of 1300 m above sea level. The instruments measuring UV radiation are installed on the roof of a building on the outskirts of the town, at Villard Saint Pancrace; they are operated by the Centre Européen Médical et Bioclimatique de Recherche et d'Enseignement Universitaire (CEMBREU). Figure 1a shows the elevation map around Briançon in a domain of 201 × 201 km^2, and Figure 1b shows the surroundings of the site, within a few kilometers. It appears that Briançon is located in a rather large valley and is surrounded by high mountains in all directions, extending at large distances, especially toward the nd south. Elevation information is taken from the Global 30 Arc Second Elevation (GTOPO30) data set, available at http://edcwww.cr.usgs.gov/landdaac/gtopo30/gtopo30.html, and it is regridded to 1 × 1 km^2. The resolution of 1 km is dictated by the resolution of the freely available GTOPO30 data set. With this resolution, distinct features such as strongly peaked mountains and deep narrow valleys will not be resolved. The 3-D results presented below are averaged over 10 × 10 pixels centered on the point of interest to reduce some numerical noise.

[8] The 3-D radiative transfer model is the Monte Carlo code for the physically correct tracing of photons in cloudy atmospheres (MYSTIC) briefly described by *Mayer* [1999, 2000]. In combination with altitude information from GTOPO30 it allows the effect of topography to be quantified for a given location. For the simulations presented here, the model domain was a square of size 201 × 201 km^2 with a resolution of 1 km. Between these data points the surface is interpolated bilinearly by MYSTIC to calculate the appropriate surface elevation and inclination at any location. The domain was centered on the station in Briançon. For the simulations a Lambertian surface albedo of 0.07 is used to resemble snow-free conditions. For completely snow-covered pixels, a value of 0.8 was used, while partly covered pixels were assigned the value of 0.3. Profiles of temperature, pressure, and ozone were taken from the U.S. Standard Atmosphere [*Anderson et al.*, 1986]. The ozone cross sections are taken from *Molina and Molina* [1986]. The ozone column was set to 340 DU (Dobson units). Neither aerosol nor clouds were included. A total of 10^9 photons were traced to give a random error in the 3-D Monte Carlo results smaller than 1%.

[9] The 1-D radiative transfer code is the successive orders of scattering (SOS). The temperature, pressure, and ozone profiles are standard midlatitude winter profiles [*McClatchey et al.*, 1972]. We have verified that the small differences with the profiles used in the 3-D model have an

Table 1. Comparison of Atmospheric Transmissions Computed With 1-D and 3-D Modeling Without Snow for Three Wavelengths

	305 nm			320 nm			340 nm		
	Global	Direct	Diffuse	Global	Direct	Diffuse	Global	Direct	Diffuse
3-D	0.0094	0.0030	0.0064	0.161	0.064	0.098	0.303	0.150	0.153
1-D	0.0095	0.0030	0.0064	0.165	0.063	0.102	0.313	0.149	0.163
1-D/3-D	1.01	1.00	1.00	1.02	0.98	1.04	1.03	0.99	1.06

influence smaller than 1% at wavelengths larger than 300 nm. As in the 3-D model the total ozone amount is fixed at 340 DU, and the *Molina and Molina* [1986] cross sections are used; the surface is Lambertian, with an albedo of 0.07 without snow. The atmosphere is divided into 22 homogeneous layers of increasing thickness between the surface and 100 km (1 km up to 5 km, 2.5 km from 5 to 30 km, 5 km from 30 to 60 km, and one single layer from 60 to 100 km). The angular integration uses a 20 point Gauss quadrature. The convergence is achieved at 1–2% after 15 iterations and even faster for a molecular atmosphere and no reflectance. The SOS code has been compared with 11 other 1-D codes for six different sets of input parameters; all the codes have been found to agree within about 2% [*Van Weele et al.*, 2000].

3. Comparison of 1-D and 3-D Models Without Snow

[10] The two models have been run for a pure molecular atmosphere (no clouds or aerosols), with a total ozone amount of 340 DU, at 305, 320, and 340 nm. The solar zenith angle (SZA) is 60°; the surface is assumed to be uniform and Lambertian, with a small albedo of 0.07. The 3-D model used the topographical information shown in Figure 1a, and results are reported for the center pixel covering the measurement station in Briançon.

[11] Comparison was done for atmospheric effective transmittances. Therefore there is no possible impact of the choice of extraterrestrial flux. Results are shown in Table 1 for the direct, diffuse, and global transmittances.

[12] At the three wavelengths the results of the 1-D code agree with the 3-D code within the expected uncertainties of a few percent for both models, with the 1-D values generally somewhat larger; however, the difference is not significant and can be explained by the minor differences in the pressure and temperature profiles used in both models, as well as by numerical and discretization small errors.

[13] Comparing the 3-D results, which include topography, with the 1-D results, we can conclude that the topography has a negligible impact on the UV irradiance when the ground surface has a low reflectance, that is, when there is no snow cover. To be more precise, the possible topography impact is too small to be detectable with the present accuracy of both measurements and modeling. Of course, topography analyzed here with 1 km resolution does not consider the possible obstruction by objects very close to the instrument site.

4. Snow Enhancement Modeled With 3-D Code

[14] In the 3-D model the snow cover has been fixed by the altitude of the snow line. The pixels above the snow line are assumed to have a Lambertian albedo of 0.8; below the snow line the albedo is, as before, 0.07; otherwise, the parameters are the same as in section 3. The enhancement is defined as the ratio of the global irradiance with snow to the global irradiance without snow, all other conditions being the same. The results of this first run are shown in Table 2 (first column for each wavelength) and Figure 2. For a given snow cover, the enhancement has similar values at 305 and 340 nm and is somewhat larger at 320 nm. This spectral behavior confirms the results obtained for uniform surfaces in 1-D modeling [*Lenoble*, 1998]; it is explained by the spectral variation of the atmosphere backscattering; therefore the enhancement in UV-B and the exact position of the maximum depend on the ozone amount and on its profile in the lower atmosphere. The snow enhancement is rather large; at 320 nm, it reaches about 38% for a snow line at 500 m and about 15% for a snow line at 2000 m.

[15] In order to isolate the influence of snow cover from the influence of topography, the 3-D model has been run with the two following assumptions, which are, of course, unrealistic but can be used to analyze the problem: (1) In run 2 the Sun is fixed at the zenith; this, of course, increases the irradiance but should not change the enhancement for a Lambertian reflectance, unless there was a strong effect of shadowing and/or of reflectances between the slopes in run 1, when the sun was at 60°; (2) in run 3 the Sun is again placed at 60° zenith angle, but the surface is assumed to be flat at the station altitude, with the same snow distribution as in the base case; this suppresses not only the shadow and reflectance effects but also the effect of a variable atmosphere thickness over the various points of the

Table 2. Influence of Topography on Enhancement by Snow for Three Wavelengths[a]

	305 nm			320 nm			340 nm		
	With Topography, SZA = 60°	With Topography, SZA = 0°	Flat Surface, SZA = 60°	With Topography, SZA = 60°	With Topography, SZA = 0°	Flat Surface, SZA = 60°	With Topography, SZA = 60°	With Topography, SZA = 0°	Flat Surface, SZA = 60°
500	1.34	1.34	1.30	1.38	1.37	1.37	1.34	1.33	1.33
1000	1.34	1.34	1.30	1.38	1.37	1.36	1.33	1.32	1.32
1500	1.27	1.27	1.23	1.30	1.29	1.29	1.26	1.25	1.25
1800	1.19	1.19	1.16	1.21	1.21	1.21	1.19	1.18	1.19
2000	1.13	1.13	1.11	1.16	1.15	1.15	1.14	1.13	1.14

[a]For each wavelength, the lumn gives the snow line altitude for cases 1 and 2; for case 3 it is just a reference for the snow cover.

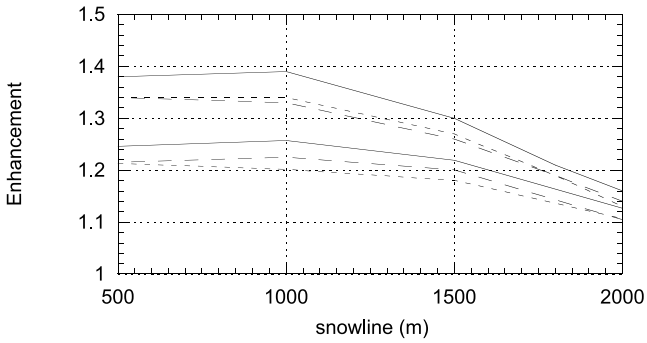

Figure 2. Enhancement versus snow line: long-dashed line, 305 nm; solid line, 320 nm; short-dashed line, 340 nm. The higher set of curves corresponds to run 1, the lower to run 4.

scene. The results of these two simulations are presented in Table 2 (first and second columns, respectively). In comparison with the results of the first run, the influence of topography appears to be negligible, around 2–3%, that is, of the order of the computation uncertainties.

[16] One could expect a larger impact of shadows when the SZA becomes larger than 60°. The 1 km resolution implies that mountain faces may be less steep in the model than in reality. This will have an effect on how much of the domain is in shadow for a given solar zenith angle. Very few pixels (0.2%) are in shadow for SZA = 60°, whereas a larger area (12.2%) is in shadow for SZA = 80°. However, the diffuse radiation is the main contributor to the global irradiance at large SZAs and UV wavelengths. For Briançon, about 90% of the global irradiance is diffuse at 340 nm and SZA = 80°. Thus the lack of direct irradiance in 12% of the pixels will have little impact on the overall UV radiation for the area. For the calculations we have adopted SZA = 60° because it is more representative for conditions under which people are outdoors during snow conditions. Furthermore, the 3-D model does not account for the Earth's curvature, which may affect the results at SZA around 80°.

[17] The snow albedo of 0.8 corresponds to a complete cover with clean fresh snow at all altitudes above the snow line; this is an extreme case, just after a snowfall. More often, at low altitude, the snow cover is only partial; in particular, trees retain snow only for a short period of time. The 3-D code has been run again (run 4) using a snow albedo of 0.3 between the tree line, fixed at 1800 m, and the snow line if it is lower than the tree line. Above the tree line (and the snow line) the albedo is 0.8; all other conditions are as in the first run. Results for the two cases (with and without a tree line) are presented in Figure 2; they will be discussed in section 5 with the experimental data.

5. Measurements of Snow Enhancement and Comparison With Modeling

[18] At the station the spectral global UV irradiance is recorded regularly every 30 min between sunrise and sunset by two spectroradiometers. The spectroradiometers are regularly intercompared. The instrument used in this study is a Jobin Yvon HD-10 spectroradiometer, scanning between 280 and 450 ith a step of 0.5 nm and a resolution of 0.7 nm; it is regularly calibrated with a 1000 W National Institute of Standards and Technology traceable standard lamp. We obtain erythemal irradiance by weighting the measured spectral irradiance with erythemal action spectrum [*McKinlay and Diffey*, 1987] and integrating over the wavelength. UV-A irradiance is calculated by integrating the spectrum from 315 to 400 nm with no weighting. A broadband Scintec radiometer provides independently erythemal UV (UV-E) and UV-A and shows good agreement with the values derived from the spectral data. For cloudless days the enhancement is therefore computed, for UV-E and UV-A, by determining the ratio of the measured values to values computed with the 1-D model for a standard clear atmosphere, with no snow on the ground, for the same solar zenith angle, and using the total ozone column provided by the Total Ozone Mapping Spectrometer (TOMS) overpass at Briançon (available at http://toms.gsfc.nasa.gov); the horizon obstruction at the instrument site reduces the diffuse irradiance by about 8–9%, and this is taken into account in the model. The 1-D model has been compared many times with measurements with no snow on the ground [*Pachart et al.*, 2000]. The model uses as input climatological aerosols [*Smolskaia et al.*, 2003]; an improvement in modeling would result from a precise knowledge of the actual aerosol content and characteristics. The method is the same as that used for the 1998 campaign. It is described in detail by *Smolskaia et al.* [2003]. The relative uncertainty in the enhancement factor was evaluated to be ±2.8% in UV-A and ±3.5% in UV-E because of the uncertainties in measured data and in the model input parameters.

[19] During winter 2002, between the beginning of January and the end of March, we observed nine very clear days, after major snowfalls. The snow line is observed visually from the station; the observation is limited between 1200 m, the lowest point in the valley, and 2400 m, which is the highest visible summit. When the snow line is given as 1200–1300 m, it means that the ground is covered with snow at the station.

[20] This visual observation is, of course, very approximate, but one must keep in mind that the notion of a snow line itself is just qualitative information about the snow cover. We have already noticed that a very extended area around the site contributes to the reflectance effect, and we will return to this point in section 6; within this large area the snow line certainly varies, depending on the exact geographical situation, the slope, and the exposition of each pixel.

[21] For all nine clear days we have analyzed between two and five spectra around local noon, depending on the quality of the data and on the atmosphere stability. These results are presented with the snow line in Figure 3; the dispersion of the data for a day is due partly to the measurement uncertainties but more likely to the natural variations, of turbidity, subvisible broken clouds, and snow reflectance. As in 1998, we find a larger enhancement in UV-E than in UV-A; this is related to the spectral variation of the enhancement shown by modeling because there is a larger contribution to UV-E than to UV-A of the wavelength range of maximum enhancement around 320 nm. However, it is difficult to quantitatively analyze this effect because of the influence of ozone both on the spectral distribution of irradiance and on the spectral variation of enhancement. Figure 3 shows, in the end of winter (March), a strong

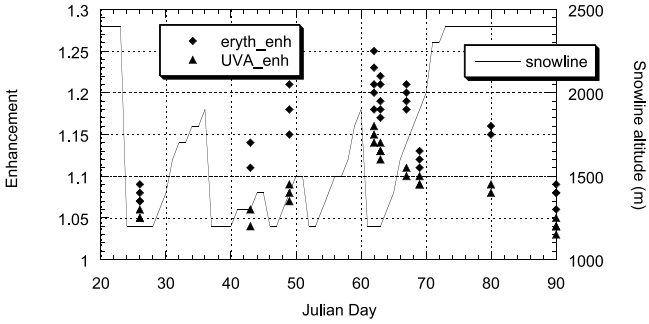

Figure 3. Snow enhancement and snow line at Briançon, 2002.

negative correlation of the enhancement with the snow line altitude. A very high enhancement is observed at the beginning of March (days 62 and 63) with a low snow line; then the snow line goes up rather regularly, and the enhancement decreases, but remains noticeable, around 5–8% at the end of the month, when the snow line is high near Briançon, but there is still a lot of snow on the summits around. At the beginning of winter the correlation between enhancement and snow line is less obvious; on day 26, with snow at the station level, the enhancement is only around 5–8%, as in the end of March with a very high snow line. This can probably be explained by the fact that the first snowfalls occurred in mid-January, and the snow cover was still sparse over most of the Alps.

[22] Figure 4 illustrates the comparison between the observed UV-E enhancement and the 3-D modeling results at 305 and 320 nm; the observed values are averaged over the several points shown in Figure 3; the model values, for each snow line altitude, are interpolated in Figure 2, for run 4, between the computation altitudes; for a snow line at 2400 m (days 80 and 90) a rough extrapolation has been performed. It appears that the 3-D modeling with an albedo of 0.3 above the snow line and below the tree line and an albedo of 0.8 at higher altitudes gives a good agreement with the UV-E measured enhancement in March, with some discrepancy on March 20 (day 80). However, we have only three good spectra on this particular day, and we use an extrapolation of model results, which is certainly less accurate than the interpolation. As already noticed and discussed above, the main disagreement is observed at the beginning of winter, that is, on 26 January and to a lesser extent on 12 February. On 26 January the enhancement appears very low, for a low snow line, with snow at the station level. The UV-A enhancement is definitively lower than the enhancement modeled at 340 nm (see Figure 3), but this can easily be understood because of the decrease of enhancement toward long wavelengths in UV-A [*Lenoble*, 1998; *Smolskaia*, 2001].

6. Retrieval of an Effective Surface Albedo

[23] For an inhomogeneous surface it is usual to define an "effective surface albedo" as the albedo of a uniform Lambertian surface that must be used as input into a 1-D model in order to reproduce the actual results. Several authors [*Kylling et al.*, 2000b; *Schmucki et al.*, 2001; *Weihs et al.*, 2001; *Smolskaia* 2003] have tried to retrieve an effective albedo, generally on the basis of measurement data, with variable success. The difficulties in retrieval of the effective albedo are generally attributed to various complex effects, such as the snow bidirectional reflectance, the slopes of the terrain, the variations of the snow characteristics, and the measurement uncertainties. Here we propose a different approach, based only on 3-D modeling results. This is of course somewhat unrealistic because the 3-D model assumes that the snow has a constant local reflectance, everywhere and at all wavelengths, and that this reflectance is Lambertian; moreover, the atmosphere characteristics are fixed by the known input data to the model. However, we hope that such an analysis can help to clarify the problem of effective albedo retrieval.

[24] We have used two different methods. The first one is straightforward and simply uses the definition of the effective albedo, with the enhancement provided by the 3-D code (section 6.1). The second method starts with the distribution of snow around the site, used in the 3-D model, with a contribution function defined in section 6.2.

6.1. Retrieval From Enhancement

[25] The relation between effective surface albedo RE and enhancement EN can easily be established using a 1-D model. The results depend on the atmosphere characteristics and on the wavelength; they are independent of SZA for the assumed Lambertian surface. Figure 5 presents this relationship computed with a 1-D code, for the site of Briançon, with the same input as used in the 3-D model. The curves are very smooth and can easily be fitted with a second-order polynomial. As noted in section 4, the results are almost the same for 305 and 340 nm, with a slightly larger enhancement at 320 nm. From the general shape of the curves it is evident that a small uncertainty in the modeled enhancement would lead to a rather large uncertainty in RE when retrieving it. This is even more obvious in the fitting equations

$$\mathrm{RE} = -4.3051 + 6.0219\mathrm{EN} - 1.6416\mathrm{EN}^2 \qquad (1a)$$

for 305 and 340 nm and

$$\mathrm{RE} = -3.7932 + 5.2714\mathrm{EN} - 1.4016\mathrm{EN}^2 \qquad (1b)$$

for 320 nm. The expected relative uncertainty of ±2% in the model values of EN leads to an absolute error of approximately ±0.05 in RE. This is a conservative

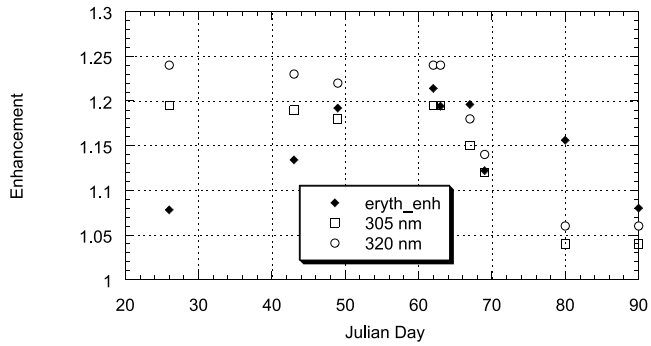

Figure 4. Measured snow enhancement compared with 3-D modeling, Briançon, 2002: observed enhancement for erythemal UV (diamonds) and modeled enhancement at 305 nm (squares) and 320 nm (circles).

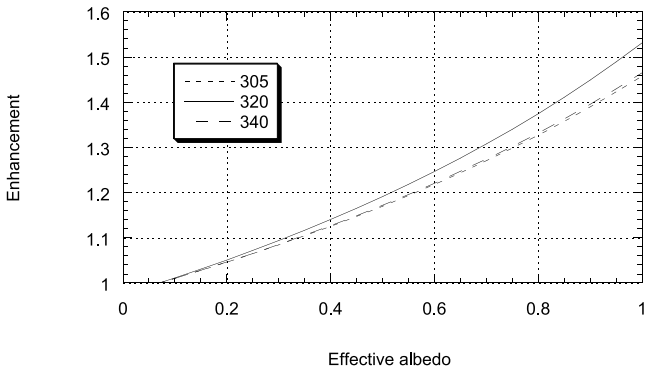

Figure 5. Snow amplification versus effective albedo from 1-D model, Briançon; ozone = 340 DU; surface reflectance = 0.07 without snow.

evaluation in comparison with the value of ±0.2 in RE, for a ±5% uncertainty in EN given by *Weihs et al.* [2001].

[26] Table 3 presents the retrieved RE at 340 nm from the model enhancement EN, calculated by the 3-D model. We have computed RE for the two runs, with topography and without topography, although we had concluded previously that the influence of topography was within the uncertainty limits of the model. This illustrates that negligible differences on EN have a nonnegligible influence on RE (reaching 0.02). For a snow line at 500 m the retrieved value of RE, with topography, is slightly larger than the obvious maximum limit of 0.8. We believe that this is explained by the effect of the expected uncertainty on EN, which should be, in this case, slightly overestimated. Reducing EN to the 1.33 value obtained without topography gives the correct value of 0.8 for RE. We have not presented the results for the two other wavelengths, as they lead to similar conclusions.

6.2. Retrieval From Snow Distribution

[27] The effective albedo can be understood as some kind of average albedo around the observation site. The problem is to define this average albedo, because the contribution of a pixel obviously depends on its distance to the site and decreases when this distance increases. For the global irradiance we have here used the method developed by *Lenoble* [2000] for the zenith sky radiance. In both cases, there is azimuthal symmetry, and the contribution $p(r)rdr$ of an element rdr depends only on its distance r to the site and not on the direction. If $\rho(r)$ is the reflectance of this element, the effective albedo is generally expressed as

$$\mathrm{RE} = \int_0^\infty \rho(r)p(r)rdr. \tag{2}$$

It is convenient to introduce an integral contribution function

$$F(R) = 2\pi \int_0^R p(r)rdr, \tag{3}$$

which represents the contribution to RE of all the pixels within a distance R from the site. We may thus discretize equation (2) as

$$\mathrm{RE} = \sum_i \rho_i[F(R_{i+1}) - F(R_i)], \tag{4}$$

where ρ_i is the surface reflectance, within the circular zone between R_i and R_{i+1}.

[28] The contribution function depends slightly on the atmospheric composition (ozone amount and profile in the lower layers, aerosol optical depth, and single-scattering albedo) and on wavelength. It does not depend on SZA for a Lambertian surface. Figure 6 presents the contribution function at 340 nm, for the standard midlatitude winter atmosphere, at Briançon altitude, with 340 DU of ozone; it has been computed with a Monte Carlo code, following the method described by *Lenoble* [2000]. The surface considered is made of a bright/dark circle of radius R within a dark/bright environment; the enhancement/reduction due to the presence of this circle, normalized to the difference between the irradiances for a complete homogeneous bright or dark surface, provides the function $F(R)$. Because of the multiple reflections between the surface and the atmosphere, $F(R)$ depends on the actual distribution of snow on the surface, and, in particular, our two cases of a bright center and a dark center give two slightly different contribution functions (see Figure 6). However, the difference is small, and we have used the average in what follows, with a simple fit:

$$F(\mathrm{R}) = 1 - \exp\left(-0.08407R + 9.46610^{-4}R^2 - 6.52710^{-6}R^3\right). \tag{5}$$

In agreement with *Degünther et al.* [1998], Figure 6 confirms that about 10% of the contribution to the enhancement is due to areas more than 40 km from the site; on the other hand, about 40% of the contribution is due to a circle of 5 km around the site, with a very rapid variation of the contribution function between 0 and 5 km.

[29] The 3-D code uses a topographical map of the area and assumes snow cover on all pixels above a fixed snow line altitude. Figure 7a presents the percentage of

Table 3. Effective Reflectance RE Retrieved From Enhancement Values EN of Table 2 at 340 nm

	EN		RE	
Snow Line Altitude for Case 1, m	Case 1 With Topography	Case 3 Without Topography	Case 1 With Topography	Case 3 Without Topography
500	1.34	1.33	0.82	0.80
1000	1.33	1.32	0.80	0.78
1500	1.26	1.25	0.68	0.66
1800	1.19	1.19	0.54	0.54
2000	1.14	1.14	0.43	0.43

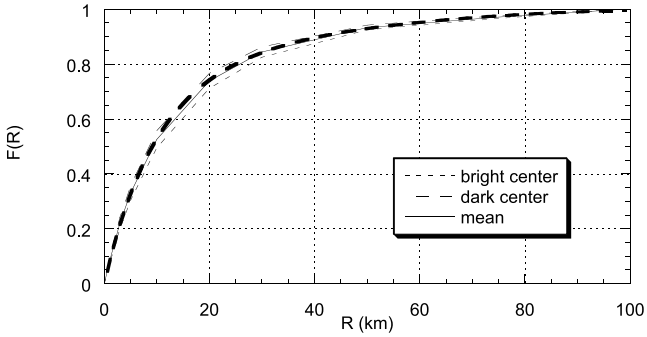

Figure 6. Integral contribution function to the 1-D effective albedo for Briançon at 340 nm. The thick dashed curve is the fit to the mean curve.

snow-covered pixels in concentric circular zones of 1 km around the Briançon site for various snow lines. In each zone we assume that the local albedo is simply the mean of the snow albedo (0.8) and of the snow-free terrain albedo (0.07), weighted by the percentage of snow-covered and snow-free pixels. Figure 7b presents this distribution of albedo, corresponding to Figure 7a. When the snow line is below 1500 m, the snow cover is very homogeneous, with a local albedo of 0.8, within the first 5 km around the station. On the other hand, when the snow line is high, at 2000 m, there is no snow near the station; the snow cover varies very rapidly in the first 5 km circle and should be known precisely because of the rapid variation of the contribution function in this zone. Unfortunately, with 1 km^2 pixels the snow cover near the station is known only very approximately.

[30] From the albedo distribution (Figure 7b), RE is computed, using equations (4) and (5). The results are given in Table 4 (second column) and are to be compared with the values of RE in the last two columns of Table 3. For a low snow line the new values of RE are a little smaller than the previous ones, but they appear somewhat better because they are just slightly smaller than 0.8, which is the limit value expected for complete snow cover. We have discussed, in section 6.1, the RE values retrieved from enhancement and concluded that, although somewhat too large for low snow lines, they are compatible with the expected uncertainty in EN. For a high snow line the values of RE retrieved here from the snow cover are higher than the previous ones retrieved from enhancement. The difference is particularly important (0.52 instead of 0.43) for a snow line at 2000 m. The agreement is better at 1800 m (0.58 instead of 0.54). In the third column of Table 4 are listed the enhancement ENs obtained using the RE values of the second column in a 1-D model, that is, deduced from Figure 5. For a snow line at 2000 m they are about 4% higher than the ENs from the 3-D model (second and third columns in Table 3), which cannot be explained by the uncertainty of ±2%. The only explanation we can propose for this discrepancy is the rough representation of snow cover associated with the rapid variation of the contribution function in the first kilometers, which is discussed above. A similar difficulty is certainly encountered when satellite images are used [*Schmucki et al.*, 2001] instead of elevation maps to retrieve an effective surface albedo from the snow cover.

7. Summary of Results

[31] We have analyzed the UV global irradiance at the Alpine site of Briançon, located in a high-altitude valley. Both 1-D and 3-D radiative transfer codes have been run with the same input data, and they have been found to give the same results, within the uncertainty of modeling (2–3%), showing no detectable influence of topography.

[32] When the ground surface is covered with snow, the 3-D model shows a strong enhancement in comparison with the case without snow, everything else being the same. Running the 3-D model with the same snow cover, but with a flat surface, gives the same enhancement within the model uncertainties; we can therefore conclude that the topography has a nondetectable influence when the surface is covered with snow as when it is free of snow.

[33] The enhancement has been measured at the Briançon station for nine cloudless days in winter 2002 for UV-E and UV-A and was found to be somewhat higher in UV-E than in UV-A; it increases as expected when the snow line altitude decreases. The 3-D model reproduces quite well the observed UV-E enhancement, reaching a maximum of about 22% in the beginning of March; this agreement is achieved, assuming a snow albedo of 0.3 above the snow line and below the tree line and of 0.8 above the tree line and the snow line. The only discrepancy appears at the beginning of the snow season (January), when the snow mantle is not well established over the Alps, and the measured enhancement remains rather low, even with snow at the station level.

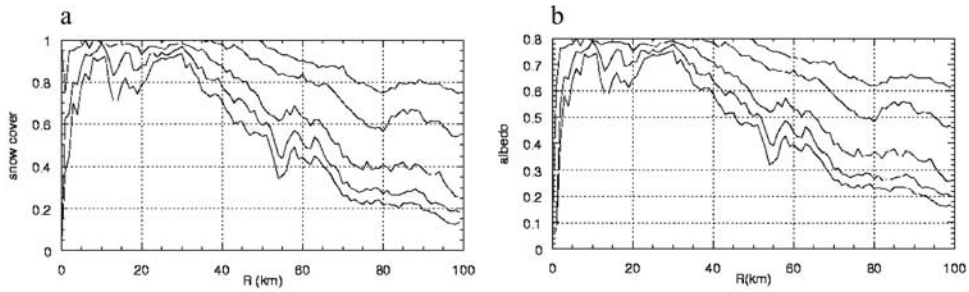

Figure 7. (a) Fraction of snow cover within circular zones between R and R + 1 km around Briançon for various snow line altitudes: (top to bottom) 500, 1000, 1500, 1800, and 2000 m. (b) Average albedo for circular zones between R and R + 1 km around Briançon for various snow line altitudes: (top to bottom) 500, 1000, 15 00, and 2000 m.

Table 4. Effective Reflectance RE Retrieved From Snow Distribution at 340 nm and Enhancement EN for This RE

Snow Line Altitude, m	RE	EN
500	0.79	1.33
1000	0.78	1.32
1500	0.68	1.27
1800	0.58	1.21
2000	0.52	1.18

From a practical point of view it is important to notice that the maximum enhancement appears at the end of winter, when the sun is already high over the horizon and the irradiance is large.

[34] The enhancement obtained from the 3-D model allows the retrieval of an effective surface albedo, that is, the albedo which should be used in order to obtain the same enhancement with a 1-D model. However, small uncertainties (±2%) in the enhancement lead to rather large uncertainties (±0.05) in the effective albedo. Another method for retrieving the effective albedo uses the distribution of the local albedo on the surface, weighted by a contribution function. The results of both methods agree when the snow line is not higher than 1500 m. For a higher snow line the snow cover is poorly represented with 1 km resolution around the Briançon site. This, together with the rapid variation of the contribution function in the first kilometers close to the site, leads to a very large uncertainty on the retrieved surface effective albedo. Our analysis confirms the difficulty observed by previous authors in retrieving a surface effective albedo by various methods [*Weihs et al.*, 2001].

[35] **Acknowledgments.** The MYSTIC model and accompanying scripts to handle GTOPO30 data were kindly provided by Bernhard Mayer. The measurements were performed at CEMBREU; we are grateful to the director, Odile Massot, and her staff and especially to Hadrien Sevray, who took care of the instrument. This work was supported by the European Commission within the project European Database for Ultraviolet Radiation Climatology and Evaluation (EDUCE).

References

Anderson, G. P., S. A. Clough, F. X. Kneizys, J. H. Chetwynd, and E. P. Shettle (1986), AFGL atmospheric constituent profiles (0–120 km), *Tech. Rep. AFGL-TR-86-0110*, Air Force Geophys. Lab., Hanscom Air Force Base, Mass.

Blumthaler, M., and W. Ambach (1988), Solar UV-B: Albedo of various surfaces, *Photochem. Photobiol.*, *48*, 85–88.

Degünther, M., R. Meerkötter, A. Albold, and G. Seckmeyer (1998), Case study on the influence of inhomogeneous surface albedo on UV irradiance, *Geophys. Res. Lett.*, *25*, 3587–3590.

Kylling, A., and B. Mayer (2001), Ultraviolet radiation in partly snow covered terrain: Observations and three-dimensional simulations, *Geophys. Res. Lett.*, *28*, 3665–3668.

Kylling, A., A. Dahlback, and B. Mayer (2000a), The effect of clouds and surface albedo on UV irradiances at a high latitude site, *Geophys. Res. Lett.*, *27*, 1411–1414.

Kylling, A., T. Persen, B. Mayer, and T. Svenøe (2000b), Determination of an effective spectral surface albedo from ground based global and direct UV irradiance measurements, *J. Geophys. Res.*, *105*, 4949–4959.

Lenoble, J. (1998), Modelling of the influence of snow reflectance on ultraviolet irradiance for cloudless sky, *Appl. Opt.*, *37*, 2441–2447.

Lenoble, J. (2000), Influence of the environment reflectance on the ultraviolet zenith radiance for cloudless sky, *Appl. Opt.*, *39*, 4247–4254.

Mayer, B. (1999), I3RC phase 1 results from the MYSTIC Monte Carlo model, paper presented at Intercomparison of 3D radiation codes (I3RC), Tucson, Ariz., November 17–19.

Mayer, B. (2000), I3RC phase 2 results from the MYSTIC Monte Carlo model, paper presented at Intercomparison of 3D radiation codes (I3RC), Tucson, Ariz., November 15–17.

Mayer, B., and M. Degünther (2000), Comment on "Measurements of erythemal irradiance near Davis Station, Antarctica: Effect of inhomogeneous surface albedo," *Geophys. Res. Lett.*, *27*, 3489–3490.

McClatchey, R. A., R. W. Fenn, J. E. A. Selby, F. E. Volz, and J. S. Garing (1972), Optical properties of the atmosphere, *Rep. AFCRL-72-0497*, Air Force Cambridge Res. Lab., Cambridge, Mass.

McKenzie, R. L., K. J. Paulin, and S. Madronich (1998), Effects of snow cover on UV irradiance and surface albedo: A case study, *J. Geophys. Res.*, *103*, 28,785–28,792.

McKinlay, A. F., and B. L. Diffey (1987), A reference action spectrum for ultraviolet induced erythema in human skin, in *Human Exposure to UV Radiation: Risks and Regulations*, edited by W. F. Passchier and B. F. Bosnajakivic, pp. 83–87, Elsevier Sci., New York.

Molina, L. T., and M. J. Molina (1986), Absolute absorption cross sections of ozone in the 185 to 350 nm wavelength range, *J. Geophys. Res.*, *91*, 14,501–14,508.

Pachart, E., J. Lenoble, C. Brogniez, D. Masserot, and J. L. Bocquet (2000), Consistency tests on UV irradiance measurements using modeling and a broadband instrument, *J. Geophys. Res.*, *105*, 4851–4856.

Schmucki, D., S. Voigt, P. Philipona, C. Fröhlich, J. Lenoble, A. Ohmura, and C. Wehrli (2001), Effective albedo derived from UV measurements in the Swiss Alps, *J. Geophys. Res.*, *106*, 5369–5383.

Smolskaia, I. (2001), Effect of inhomogeneous surface albedo on UV radiation in the Antarctic environment, Ph.D. thesis, Univ. of Tasmania, Hobart, Australia.

Smolskaia, I., M. Nuñez, and K. Michael (1999), Measurements of erythemal irradiance near Davis Station, Antarctica: Effect of inhomogeneous surface albedo, *Geophys. Res. Lett.*, *26*, 1381–1384.

Smolskaia, I., D. Masserot, J. Lenoble, C. Brogniez, and A. de La Casinière (2003), Retrieval of the ultraviolet effective snow albedo during 1998 winter campaign in the French Alps, *Appl. Opt.*, *42*, 1583–1587.

Van Weele, M., et al. (2000), From model intercomparison toward benchmark UV spectra for six real atmospheric cases, *J. Geophys. Res.*, *105*, 4915–4925.

Weihs, P., S. Simic, W. Laube, W. Mikielewicz, G. Rengarajan, and M. Mandl (1999), Albedo influences on surface UV irradiance at the Sonnblick high mountain Observatory (3106 m altitude), *J. Appl. Meteorol.*, *38*, 1599–1610.

Weihs, P., et al. (2001), Modeling the effect of an inhomogeneous surface albedo on incident UV radiation in mountainous terrain: Determination of an effective surface albedo, *Geophys. Res. Lett.*, *28*, 3111–3114.

A. Kylling, NILU-Kjeller, P.O. Box 100, N-2027 Kjeller, Norway. (arve.kylling@nilu.no)

J. Lenoble, Laboratoire d'Optique Atmosphérique, UMR 8518, Université des Sciences et Technologies de Lille, F-59655 Villeneuve d'Ascq, France. (jacqueline.lenoble@loa.univ-lille1.fr)

I. Smolskaia, Institute for Meteorology and Climatology, University of Hannover, Herrenhäuser Strasse 2, D-30419 Hannover, Germany. (smolskaia@muk.uni-hannover.de)